



SCIENTIFIC OASIS

Journal of Intelligent Decision Making
and Granular Computing

Journal homepage: www.jidmag.org

ISSN: 3042-3759



Adaptive Robust Control Schemes for an Uncertain 2-dof Manipulator Subjected to Disturbances

Kaili Zhao¹, Tong Song^{2,3}, BinBin Ai^{4,*}

¹ Binzhou Polytechnic, Binzhou, Shandong 256600, China

² No.3 Middle School of Qihe, Dezhou, Shandong 251100, China

³ School of Mathematics Science Liaocheng University, Liaocheng, Shandong 252000, China

⁴ Agricultural Development Bank of China Bijie Branch, Bijie, Guizhou 551799, China

ARTICLE INFO

Article history:

Received 14 August 2025

Received in revised form 28 September 2025

Accepted 20 October 2025

Available online 24 October 2025

Keywords:

Adaptive control; Robotic manipulator; Neural networks

ABSTRACT

This paper focuses on the tracking problem for a 2-link rigid robotic manipulator with model uncertainties and disturbances. The manipulator is always subject to disturbances such as environmental disturbance, measurement noise, and so forth, which makes the controller design a far more complex task. By combining the “core function” with a neural network, the deep-rooted information of the system uncertainties can be extracted and then further compensated by a robust method. In addition, in this paper, the disturbance is formulated as a norm-bounded variable, and thus the adaptive robust controllers based on backstepping design and filtered variables are developed simultaneously. Finally, simulation studies show the effectiveness of the control algorithms..

1. Introduction

Manipulators are widely used in various industrial scenarios. Fig. 1 summarizes several representative applications, including intelligent manufacturing, hazard mitigation, and lifting operations. Fig. 1(c) and (d) present typical examples of heavy-duty manipulators: the former, referred to as articulated cranes, manipulates joint angles to lift a platform to a specified height, whereas the latter is commonly employed in ports for oil and gas transportation [1–5].

Over the past decades, the tracking problem of manipulators has attracted considerable attention. The development of tracking controllers is challenging because of nonlinear system dynamics, input constraints (e.g., backlash, dead zones, and saturation), and the complexities introduced by unmodeled dynamics and closed-chain mechanisms, particularly as the number of degrees of freedom (DoF) increases [6]. Numerous studies have investigated the control problems of manipulators

*Corresponding author.

E-mail address: aibinbin@adbc.com.cn

<https://doi.org/10.31181/jidmgc11202520>

© The Author(s) 2025 | [Creative Commons Attribution 4.0 International License](https://creativecommons.org/licenses/by/4.0/)

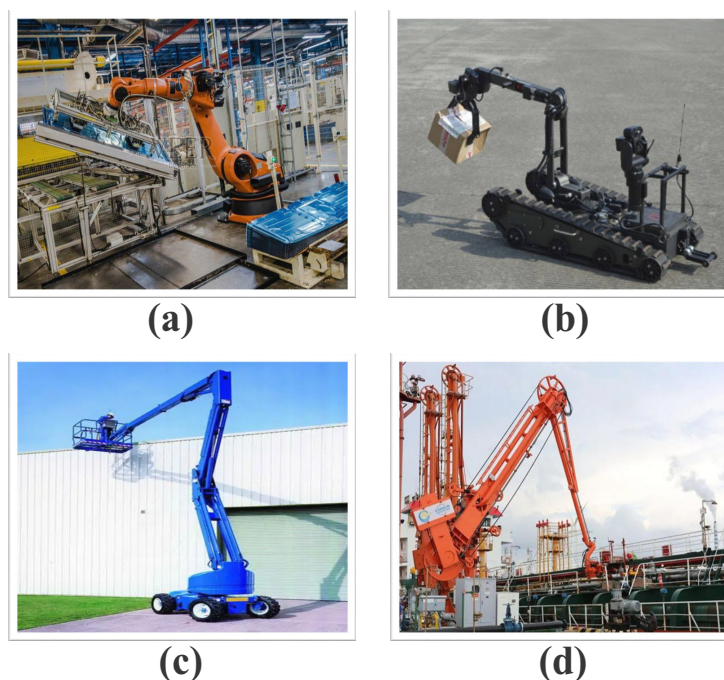


Fig 1. typical application scenarios.

in free-motion tasks. A variety of approaches have been proposed for joint motion control, including adaptive control [7], adaptive robust control [8], neuroadaptive backstepping sliding-mode control [9], and model predictive control [10]. In [11], the Euler-Lagrange systems was studied well subjected to nonparametric uncertainties, and zero-error tracking controller was developed by using a speed function. Intelligent control strategies, such as reinforcement learning [12] and radial basis function neural networks [13], have also been explored.

The use of neural networks (NNs) to handle model uncertainties is a widely adopted approach [14], since it has been proven that NNs can approximate nonlinear functions with arbitrary accuracy under suitable conditions [15]. For example, in [16], an NN was employed to compensate for dynamic uncertainties, and in [17], NN-based controllers were utilized to achieve tracking control in the presence of uncertainties for an n -link flexible-joint manipulator. The core idea of NN-based control design within Lyapunov's stability framework is to construct an adaptive law for each element of the weight vector and to incorporate the approximation error into the Lyapunov function, thereby estimating the ideal weight vector. Therefore, when the unknown function is highly complex, the number of neural network nodes must be increased to enhance the approximation, which significantly enlarges the dimension of the adaptive parameters. Consequently, the online learning time may become prohibitively long.

Disturbances are inevitable factors that limit system performance and may even affect system stability, particularly when the system is also subject to uncertainties. In fact, disturbances can arise from a variety of sources, such as internal noise, unmodeled dynamics, and other factors. Depending on their source, disturbances can also be represented by different mathematical formulations, such as external system models or norm-bounded variables [18]. An operating manipulator is often affected by multiple types of disturbances, referred to as multiple disturbances. For disturbances that originate from external system models, disturbance observer (DO)-based control is an effective approach. The main idea is to construct an observer to estimate the disturbance and then feed this estimate back into the servo system in real time, thereby enabling disturbance compensation [19–22] However, DO-based methods often require precise model information, which introduces conservatism into the proposed approaches.

Motivated by these discussions, in this paper, we employ a DO-based adaptive robust control design to deal with the problem of trajectory tracking via neural-network control design for a 2-link manipulator in the presence of multiple disturbances and uncertainties. The main contributions of this paper are summarized as follows:

- 1) Combining the “core function” with neural network, an effective adaptive updating algorithm is proposed, which can not only compensate the uncertainty of the system well, but also reduce computational burden greatly.
- 2) A novel control method based on filtering variables (FV) is proposed. Different from the back-stepping method, the proposed control design can achieve effective tracking without introducing virtual control signals (see 3.2), thus reducing the complexity of controller.

2. Problem Formulation

2.1 System model without uncertainties:

The dynamic equation of an 2-link rigid manipulator system (see Fig. 2) can be described as

$$M(q)\ddot{q} + C(q, \dot{q})\dot{q} + G(q) = \tau(t) - f(t), \quad (1)$$

where $q = [q_1, q_2]^T$, $\dot{q} = [\dot{q}_1, \dot{q}_2]^T$, and $\ddot{q} = [\ddot{q}_1, \ddot{q}_2]^T$ represent the angle position, velocity, and acceleration, respectively. $\tau(t) = [\tau_1(t), \tau_2(t)]^T$ denote the control input. $M(q) \in \mathcal{R}^{2 \times 2}$ is the inertia matrix which is symmetric and positive definite, $C(q, \dot{q}) \in \mathcal{R}^{n \times n}$ is the centripetal and Coriolis matrix, $G(q) \in \mathcal{R}^n$ is the vector of gravitational force, and $f(t) \in \mathcal{R}^n$ represents the multiple disturbance, which comes from modelling error, system noises and uncertainties. The detailed expressions of M, C, G are as follows

$$M = \begin{bmatrix} M_{11} & M_{12} \\ M_{21} & M_{22} \end{bmatrix}, C = \begin{bmatrix} C_{11} & C_{12} \\ C_{21} & C_{22} \end{bmatrix}, G = \begin{bmatrix} G_1 \\ G_2 \end{bmatrix}.$$

where $M_{11} = m_1 l_{c1}^2 + m_2(l_1^2 + l_{c2}^2 + 2l_1 l_{c2} \cos(q_2)) + I_1 + I_2$, $M_{12} = M_{21} = m_2(l_{c2}^2 + l_1 l_{c2} \cos(q_2)) + I_2$, $M_{22} = m_2 l_{c2}^2 + I_2$, $C_{11} = -m_2 l_1 l_{c2} \dot{q}_2 \sin(q_2)$, $C_{12} = -m_2 l_1 l_{c2} (\dot{q}_1 + \dot{q}_2) \sin(q_2)$, $C_{21} = m_2 l_1 l_{c2} \dot{q}_1 \sin(q_2)$, $C_{22} = 0$, $G_1 = (m_1 l_{c1} + m_2 l_1)g \cos(q_1) + m_2 l_{c2} g \cos(q_1 + q_2)$ and $G_2 = m_2 l_{c2} g \cos(q_1 + q_2)$.

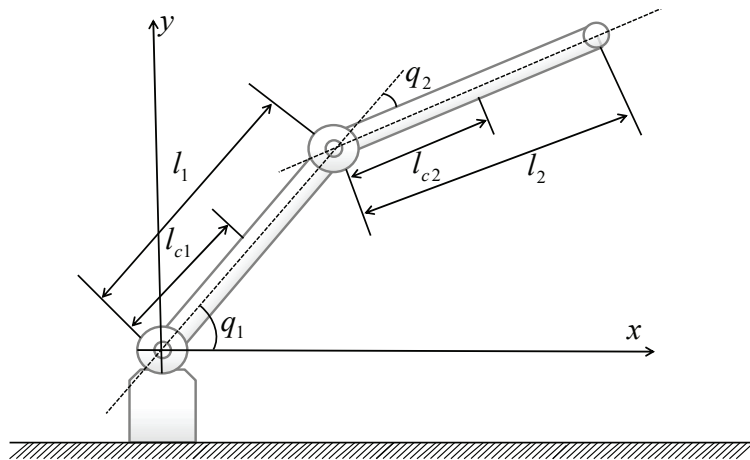


Fig 2. Robot manipulator.

Choosing $x_1 = q$ and $x_2 = \dot{q}$ yields the equivalent form of system (1)

$$\begin{aligned} \dot{x}_1 &= x_2 \\ \dot{x}_2 &= M^{-1}[\tau - f - Cx_2 - G]. \end{aligned} \quad (2)$$

The control objective of this paper is to design control inputs with adaptive NN law to satisfy the following criteria

\mathcal{Q}_1 : All signals of the closed-loop system are bounded.

\mathcal{Q}_2 : The output $q(t)$ can follow the desired trajectory x_d .

The following mild hypothesis assumptions and technical lemmas are presented to help to achieve the control purposes.

Assumption 1: There exists a constant ω such that $\|f\| \leq \omega$.

Assumption 2: The desired trajectory x_d is continuous and bounded, and its first and second derivative are also continuous.

Lemma 1[17]: Consider system $\dot{\chi} = f(\chi)$, and assume there exist $\Delta > 0$, positive definite function $V(x)$, two functions β_1 and β_2 belong to κ_∞ , real numbers $c > 0$ such that

$$\begin{aligned}\beta_1(|x|) &\leq V(x) \leq \beta_2(|x|), \\ \dot{V} &\leq -cV(x) + \Delta,\end{aligned}\tag{3}$$

for all $\chi \in \mathbb{R}^n$, then, (i). All $\chi(t) \in \mathbb{R}^n$ are bounded. (ii). $\chi(t)$ will remain in the compact $\Omega = \{\chi(t) \leq \sqrt{V(0) + \frac{\Delta}{c}}\}$, and satisfy $\lim_{t \rightarrow \infty} |\chi(t)| \leq \sqrt{\frac{\Delta}{c}}$.

Lemma 2[16]: Matrices M and C satisfy $\forall x \in \mathbb{R}^n, x^T(\dot{M} - 2C)x = 0$.

2.2 System model with uncertainties and Neural Networks:

Limited by economic cost and measurement technology, the matrices M, G, C of system (2) is generally difficult to construct accurately in practice, and G, C can be written as $C = \bar{C} + \Delta C$ and $G = \bar{G} + \Delta G$, where $\bar{\cdot}$ is the known part and $\Delta \cdot$ is the unknown part. Then 2 can be rewritten as with the system uncertainties,

$$\begin{aligned}\dot{x}_1 &= x_2 \\ \dot{x}_2 &= M^{-1}[\tau - \bar{C}x_2 - \Delta Cx_2 - \bar{G} - \Delta G - f].\end{aligned}\tag{4}$$

Considering the tracking errors $z_1 = x_1 - x_d$ and $z_2 = x_2 - \alpha$, where α is the virtual controller and will be designed later, the system 4 can be rewritten as

$$\begin{aligned}\dot{z}_1 &= z_2 \\ \dot{z}_2 &= M^{-1}[\tau - Cz_2 - \bar{C}\alpha - \bar{G} + \mu - f + M\dot{\alpha}].\end{aligned}\tag{5}$$

where $\mu = -\Delta C\alpha - \Delta G - M\dot{\alpha} \in \mathbb{R}^2$.

In the following control design, M can not be used by controller, and radial basis function neural network (RBFNN) will be used to estimate unknown function μ . In fact, for any continuous function $h(x)$, it can be represented as

$$h(x) = W^T S(x) + \epsilon,$$

where $W = [W_1, W_2, \dots, W_N]^T \in \mathbb{R}^N$ is the weight vector and $\epsilon > 0$ denotes the approximation error. $S(x) = [S_1(x), \dots, S_N(x)]^T$ with the NN node number $N > 1$, and can be chosen as the Gaussian functions as:

$$S_i(x) = \exp\left[-\frac{\|x - \iota_i\|^2}{\lambda_i}\right], i = 1, \dots, N$$

where $\iota_i \in \mathbb{R}^n$ is the center with $\lambda_i \in \mathbb{R}^n$ being width.

Lemma 3[11]: The RBFNN approximation error ϵ is bounded, i.e. $|\epsilon| \leq \epsilon_*$, where ϵ_* is an unknown constants.

3. Control Design

3.1 Backstepping-based Control

In the following, NN-based backstepping controller is provided.

Step 1: We construct the candidate Lyapunov function as

$$V_1 = \frac{1}{2} z_1^T z_1.$$

Differentiating V_1 yields that

$$\begin{aligned} \dot{V}_1 &= z_1^T (z_2 + \alpha - \dot{x}_d) \\ &\leq \frac{1}{2} z_1^T z_1 + \frac{1}{2} z_2^T z_2 + z_1^T (\alpha - \dot{x}_d). \end{aligned} \quad (6)$$

Take the virtual controller as

$$\alpha_1 = \dot{x}_d - \frac{1 + 2r_1}{2} z_1, \quad (7)$$

where $r_1 > 0$ is a design parameter. From (6) and (7), we have

$$\dot{V}_1 \leq -r_1 z_1^T z_1 + \frac{1}{2} z_2^T z_2. \quad (8)$$

Step 2: Consider the candidate Lyapunov function as

$$V_2 = V_1 + \frac{1}{2} z_2^T M z_2 + \frac{1}{2} \tilde{W}^T \tilde{W},$$

where $\tilde{W} = W - \hat{W}$, and \hat{W} is the estimation of W , and $W = [W_1, W_2]^T$ and $\begin{bmatrix} W_1 & W_2 \end{bmatrix} \begin{bmatrix} S_1 \\ S_2 \end{bmatrix} + \begin{bmatrix} \epsilon_1 \\ \epsilon_2 \end{bmatrix} = \mu$. Taking the derivative of V_2 , one obtains the following expression

$$\begin{aligned} \dot{V}_2 &= \dot{V}_1 + z_2^T M \dot{z}_2 + z_2^T \dot{M} z_2 - \tilde{W}^T \dot{\tilde{W}} \leq -r_1 z_1^T z_1 \\ &\quad + \frac{1}{2} z_2^T z_2 + z_2^T (\tau - \overline{C}\alpha - \overline{G} + \mu - f) - \tilde{W}^T \dot{\tilde{W}}. \end{aligned}$$

Recalling that $\|f\| \leq \theta$, then we design the control input τ and the adaption law $\dot{\hat{W}}$ and $\dot{\hat{\theta}}$ as

$$\begin{aligned} \tau &= -\frac{1 + 2r_2}{2} z_2 + \overline{C}\alpha + \overline{G} - \hat{W}^T S \\ &\quad - 2l_1 (\hat{\theta} + \frac{1}{2}) z_2 \\ \dot{\hat{W}} &= z_2^T S - \sigma_1 \hat{W} \\ \dot{\hat{\theta}} &= 2l_1 z_2^T z_2 - \sigma_2 \hat{\theta} \end{aligned} \quad (9)$$

Then time derivative of V_2 satisfies

$$\begin{aligned} \dot{V}_2 &\leq -r_1 z_1^T z_1 - r_2 z_2^T z_2 - l_1 z_2^T z_2 - z_2^T f \\ &\quad - 2l_1 z_2^T z_2 \hat{\theta} + \sigma_1 \tilde{W}^T \hat{W} + z_2^T \epsilon \end{aligned} \quad (10)$$

Using Young's inequality obtains

$$\begin{aligned} -z_2^T f &\leq 2l_1 z_2^T z_2 \theta + \frac{1}{2l_1} \\ z_2^T \epsilon &\leq l_1 z_2^T z_2 + \frac{\epsilon_*^2}{4l_1} \end{aligned}$$

Then (10) can be rewritten as

$$\begin{aligned} \dot{V}_2 &\leq -r_1 z_1^T z_1 - r_2 z_2^T z_2 + 2l_1 z_2^T z_2 \theta - 2l_1 z_2^T z_2 \hat{\theta} \\ &\quad + \sigma_1 \tilde{W}^T \hat{W} + \frac{1}{2l_1} + \frac{\epsilon_*^2}{4l_1} \end{aligned} \quad (11)$$

$-\frac{1}{2}\sigma_1 \tilde{W}^T \tilde{W} + \frac{1}{2}\sigma_1 W^T W + \sigma_2 \tilde{\theta}^T \hat{\theta}$. Now one can give the first result in the following theorem.

Theorem 1: Suppose the (2) satisfies Assumption 1-2. Then, the NN-based adaptive controller (10) can guarantee the control objectives $\mathcal{O}_1 - \mathcal{O}_2$ achieved.

proof: We design the Lyapunov functional candidate as

$$V = V_2 + \frac{1}{2}\tilde{\theta}^2, \quad (12)$$

where $\tilde{\theta} = \theta - \hat{\theta}$. Then using (9) and (10), it can simply obtain

$$\begin{aligned} \dot{V} &\leq -r_1 z_1^T z_1 - r_2 z_2^T z_2 + \sigma_1 \tilde{W}^T \hat{W} \\ &\quad + \sigma_2 \tilde{\theta}^T \hat{\theta} + \frac{1}{2l_1} + \frac{\epsilon_*^2}{4l_1} \end{aligned} \quad (13)$$

Note that the following inequality holds

$$\begin{aligned} \sigma_1 \tilde{W}^T \hat{W} &= \sigma_1 \tilde{W}^T (W - \tilde{W}) \\ &\leq \sigma_1 \left(-\frac{1}{2} \tilde{W}^T \tilde{W} + \frac{1}{2} W^T W \right) \\ \sigma_2 \tilde{\theta}^T \hat{\theta} &= \sigma_2 \tilde{\theta}^T (\theta - \tilde{\theta}) \\ &\leq \sigma_2 \left(-\frac{1}{2} \tilde{\theta}^T \tilde{\theta} + \frac{1}{2} \theta^T \theta \right) \end{aligned}$$

By substituting the above inequalities into (13) has

$$\begin{aligned} \dot{V} &\leq -r_1 z_1^T z_1 - r_2 z_2^T z_2 - \frac{1}{2}\sigma_1 \tilde{W}^T \tilde{W} - \frac{1}{2}\sigma_2 \tilde{\theta}^T \tilde{\theta} \\ &\quad + \frac{1}{2}\sigma_1 W^T W + \frac{1}{2}\sigma_2 \theta^T \theta + \frac{1}{2l_1} + \frac{\epsilon_*^2}{4l_1} \\ &\leq -cV + \Delta \end{aligned} \quad (14)$$

where $c = \min\{2r_1, \frac{2r_2}{\lambda_{\min}(M)}, 2\sigma_1, 2\sigma_2\}$ and $\Delta = \frac{1}{2}\sigma_1 W^T W + \frac{1}{2}\sigma_2 \theta^T \theta + \frac{1}{2l_1} + \frac{\epsilon_*^2}{4l_1}$. Using Lemma 1, it can be concluded that the control objectives \mathcal{O}_1 and \mathcal{O}_2 are achieved, which complete the proof of Theorem 1.

3.2 FV-based Control

In this section, the control strategy filtering variables will be proposed. Firstly, a novel filtering variable is defined as $s = \beta_1 e + \dot{e}$, where $e = x - x_d$, $x = q$, and $\beta_1 > 0$. Then we rewrite system (1) as

$$\ddot{x} = M^{-1}(\tau - f) + M^{-1}(-C\dot{x} - G). \quad (15)$$

Differentiating s gets $\dot{s} = M^{-1}(\tau - f) + M^{-1}(-C\dot{x} - G) + L$, where $L = \ddot{y}_d + \beta_1 \dot{e}$. In order to solve computational resources, we further generalize Lemma 4 as follows.

Lemma 4: For any continuous function $h(x)$ in, one further has

$$\begin{aligned} h(x) &\leq \|W^T\| \|S(x)\| + \epsilon_* \\ &\leq a\varphi(x) \end{aligned}$$

where $a = \max\{\|W^T\|, \epsilon_*\}$ and $\varphi(x) = \|S(x)\| + 1$. The remaining control design is divided into two steps.

Step 1: Consider the candidate Lyapunov function as

$$V_1 = \frac{1}{2} s^T M s \quad (16)$$

Similar to 3.1, one has

$$\begin{aligned} \dot{V}_1 &= s^T M \dot{s} + \frac{1}{2} s^T \dot{M} s \\ &= s^T (\tau - f - C\dot{x} - G + Cs) + s^T ML. \end{aligned}$$

To account for system uncertainties, \dot{V}_1 should be rewritten as

$$\begin{aligned} \dot{V}_1 &= s^T (\tau - f - \bar{C}\dot{x} - \Delta C\dot{x} - \bar{G} - \Delta G \\ &\quad + \bar{C}s + \Delta Cs + \bar{M}L + \Delta ML) \\ &= s^T (\tau - f - \bar{C}\dot{x} - \bar{G} + \bar{C}s \\ &\quad + \bar{M}L + \bar{\mu}), \end{aligned} \quad (17)$$

where $\bar{\mu} = -\Delta C\dot{x} - \Delta G + \Delta Cs + \Delta ML$.

Since $\|\bar{\mu}\|$ is continuous, then with the help of Lemma 5 and Cauchy-Buniakowsky-Schwarz inequality, we have

$$\begin{aligned} s^T \bar{\mu} &\leq \|s\| \|\bar{\mu}\|, \\ &\leq \|s\| a\varphi. \end{aligned} \quad (18)$$

Design the controller and the adaption laws as

$$\begin{aligned} \tau &= -r_1 s + \bar{C}\dot{x} + \bar{G} - \bar{C}s - \bar{M}L \\ &\quad - \frac{2s\hat{\theta}^2}{\sqrt{\|s\|^2 \hat{\theta}^2 + o(t)^2}} - \frac{s\hat{a}^2 \varphi^2}{\sqrt{\|s\|^2 \hat{a}^2 \varphi^2 + o(t)^2}} \\ \dot{\hat{a}} &= 2\|s\| \\ \dot{\hat{\theta}} &= \|s\| \varphi. \end{aligned} \quad (19)$$

where $\hat{\theta}$ and \hat{a} are the estimations of θ and a . $o(t)$ is a positive function which satisfies $\int_0^t o(s)ds < \lim_{t \rightarrow +\infty} \int_0^t o(s)ds < o_*$, where $o_* > 0$ is a constant.

Now, we can give the second result of this paper.

Theorem 2: Considering system (1) under Assumptions 1-2, if the control law and adaptive laws are designed as (19), the control objectives $Q_1 - Q_2$ can be guaranteed.

proof: One picks up the candidate Lyapunov function as

$$V = V_1 + \frac{1}{2}\tilde{a}^2 + \frac{1}{2}\tilde{\theta}^2 \quad (20)$$

where $\tilde{a} = a - \hat{a}$ and $\tilde{\theta} = \theta - \hat{\theta}$. The derivative of V gives

$$\dot{V} = \dot{V}_1 - \tilde{a}\dot{\hat{a}} - \tilde{\theta}\dot{\hat{\theta}}$$

Substitute τ and (19) into \dot{V} gets

$$\begin{aligned} \dot{V} &= \dot{V}_1 - \tilde{a}\dot{\hat{a}} - \tilde{\theta}\dot{\hat{\theta}} \\ &\leq -s^T(f_d + \tilde{f}) - \frac{2\|s\|^2\hat{\theta}^2}{\sqrt{\|s\|^2\hat{\theta}^2 + o(t)^2}} + \|s\|a\varphi \\ &\quad - \frac{\|s\|^2\hat{a}^2\varphi^2}{\sqrt{\|s\|^2\hat{a}^2\varphi^2 + o(t)^2}} - \tilde{a}\dot{\hat{a}} - \tilde{\theta}\dot{\hat{\theta}} - r_1s^Ts \\ &\leq 2\|s\|v + \|s\|a\varphi - \frac{2\|s\|^2\hat{\theta}^2}{\sqrt{\|s\|^2\hat{\theta}^2 + o(t)^2}} - r_1s^Ts \\ &\quad - \frac{\|s\|^2\hat{a}^2\varphi^2}{\sqrt{\|s\|^2\hat{a}^2\varphi^2 + o(t)^2}} - \tilde{a}\dot{\hat{a}} - \tilde{\theta}\dot{\hat{\theta}} \end{aligned} \quad (21)$$

Note that

$$\begin{aligned} -\frac{2\|s\|^2\hat{\theta}^2}{\sqrt{\|s\|^2\hat{\theta}^2 + o(t)^2}} &\leq -2\|s\|\hat{\theta} + 2o(t) \\ -\frac{\|s\|^2\hat{a}^2\varphi^2}{\sqrt{\|s\|^2\hat{a}^2\varphi^2 + o(t)^2}} &\leq -\|s\|\hat{a}\varphi + o(t). \end{aligned}$$

Then one further has

$$\begin{aligned} \dot{V} &\leq 2\|s\|\tilde{\theta} + \|s\|\tilde{a}\varphi + 3o(t) - r_1s^Ts \\ &\quad - \tilde{a}\dot{\hat{a}} - \tilde{\theta}\dot{\hat{\theta}} \\ &\leq -r_1s^Ts + 3o(t). \end{aligned} \quad (22)$$

Integrating (22) over $[0, t]$ gets

$$V(t) + r_1 \int_0^t s^Ts d\tau \leq 3o_*. \quad (23)$$

It can be concluded that $V(t) \in L_\infty$, which means all signals in the closed loop system 1. Based on this result, one obtains that $\dot{s}(t) \in L_\infty$. Since that $e_j(t) \in L_2$, then, by using Babalat's Lemma, we know that $\lim_{t \rightarrow \infty} s(t) = 0$, which implies that objective $Q_1 - Q_2$ are achieved.

Remark 1 The design of 3.1 is a bounded control, that is, the tracking error is globally uniformly bounded, while FV-based control can achieve zero error control, i.e. the tracking error is asymptotically stable.

Remark 2 In terms of both controller structure and computational effort, FV-based methods provide a streamlined and efficient alternative to backstepping, making them particularly attractive for real-time applications.

4. Simulation Results

To exemplify the effectiveness of the proposed control scheme, we consider the robotic manipulator system with the following (Tab. 1) physical parameters.

Table 1: Parameters of the manipulator.

Parameter	Description	Value
m_1	the mass of link 1	2.0 kg
m_2	the mass of link 2	0.85 kg
l_1	the length of link 1	0.35 m
l_2	the length of link 2	0.31 m
I_1	the inertia of link 1	$61.25 \times 10^{-3} \text{ kgm}^2$
I_2	the inertia of link 2	$20.42 \times 10^{-3} \text{ kgm}^2$
g	the earth acceleration	9.8 m/s^2

Assuming that only 60%' information of matrix C, G, M are known, and the reference signal is given as $x_d = [\sin(t), \cos(t)]^T$. The mutiple disturbances is set as $f = f_s + f_d$, where f_s comes from $f_s = F\omega$ and $f_d = [0.1 \sin(t), 0.1 \cos(t)]^T$. In addition, $\dot{\omega} = \mathcal{M}\omega$, and $\mathcal{M} = \begin{pmatrix} -0.5 & 0 \\ 0 & -0.1 \end{pmatrix}$ and $F = \begin{pmatrix} 10 & 20 \\ 5 & 6 \end{pmatrix}$.

4.1 Backstepping-based Control

In this part, we simulate the algorithm in 3.1. The control parameters are selected as $r_1 = 10$, $r_2 = 10$, $l_1 = 0.3$, $\sigma_1 = 0.002$, $\sigma_2 = 0.1$. The initial value of system are set as $x_1(0) = [0.3, 0.7]^T$, $x_2(0) = [0, 0]^T$, $\dot{W}(0) = 0$, and $\hat{\theta}(0) = 0$. It is seen from Fig. 3 that the desired tracking goal is achieved and all states are bounded. Fig. 4-5 show the tracking errors, and Fig. 6 illustrates the approximation of the $\mu = [\mu_1, \mu_2]$ by RBFNNs. Fig. 7 displays adaptive parameters and Fig. 8 gives the control signals.

4.2 FV-based Control

In this section, we choose the same initial values of the system as 4.1 with $\hat{a} = \hat{\theta} = 0.5$, $r_1 = \beta_1 = 10$, and $o(t) = \exp(-0.2t)$. For simplicity, denote q as $x_1 = [x_{11}, x_{12}]^T$ and \dot{q} as $x_2 = [x_{21}, x_{22}]^T$. The simulation results can be seen in Figs. 9-13. Fig. 9 shows the excellent tracking performance of the FV-based control. From Figs. 3-5 and Figs. 8-10, it can be concluded that a higher tracking precision can be achieved by using FV-based control, which supports the **Remark 1**. It can be seen from Fig. 11 that $\|\bar{\mu}\| \leq \hat{a}\varphi$ holds as time goes by, which implies that the adaptive parameter \hat{a} can estimate a well. The adaptive parameters $\hat{\theta}$ and \hat{a} are given by Fig. 12. Fig. 13 shows the control signals.

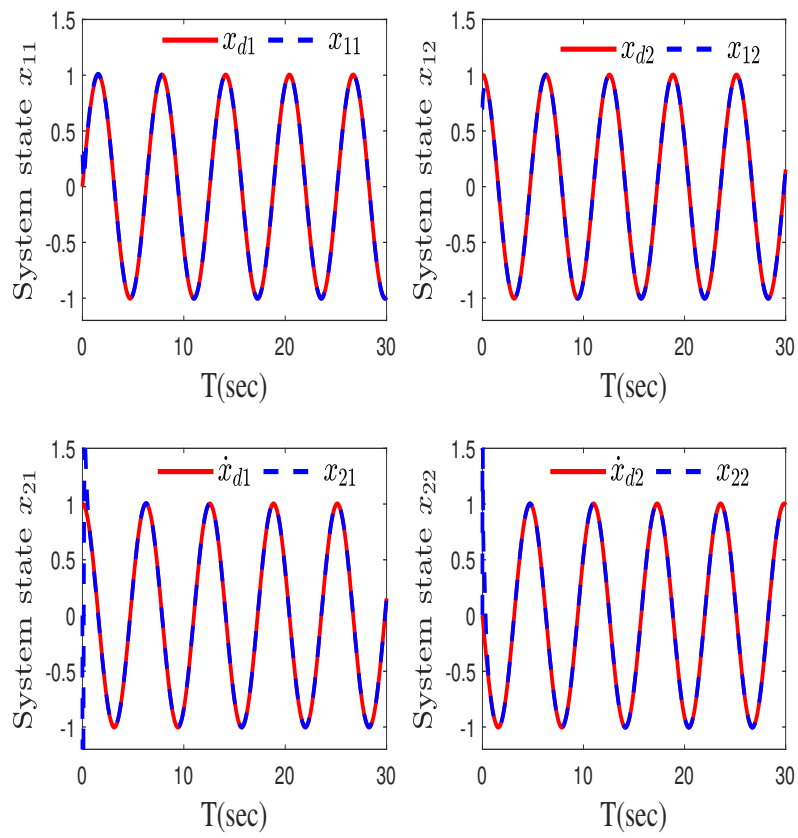


Fig 3. System states.

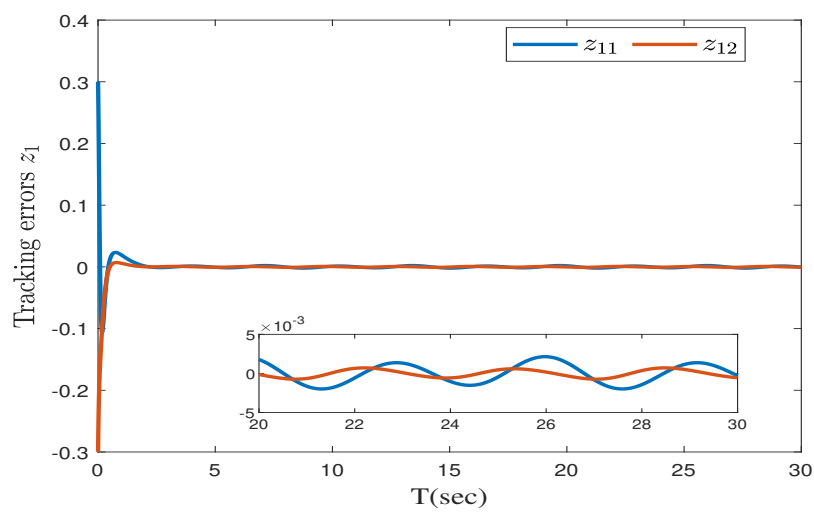


Fig 4. Tracking error z_1 .

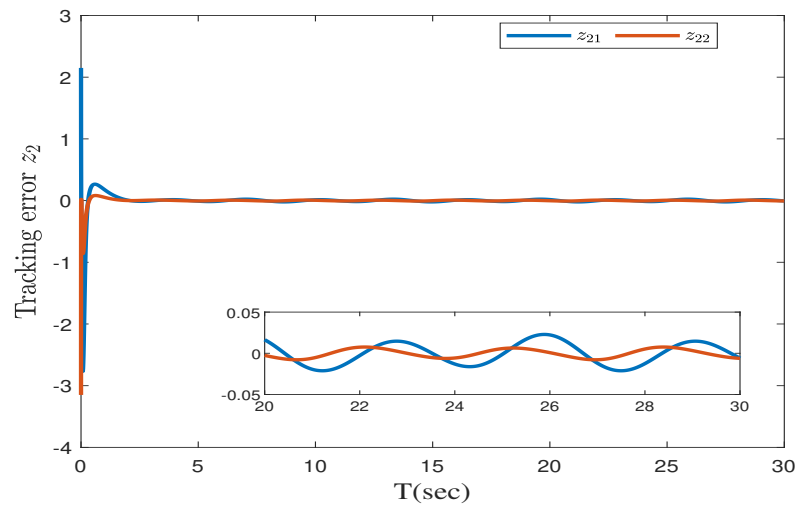


Fig 5.Tracking error z_2 .

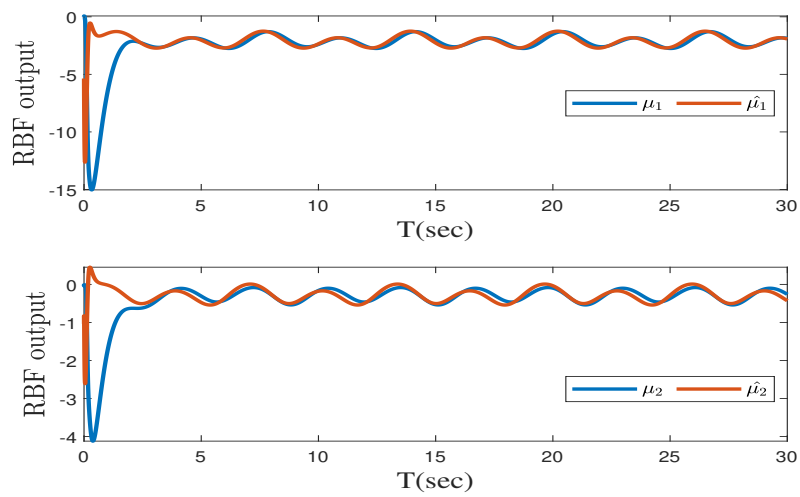


Fig 6. μ and its approximation.

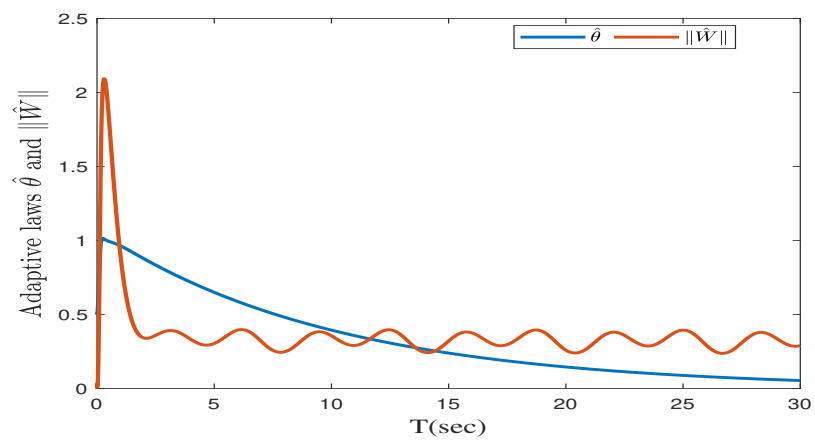


Fig 7. Adaptive parameters.

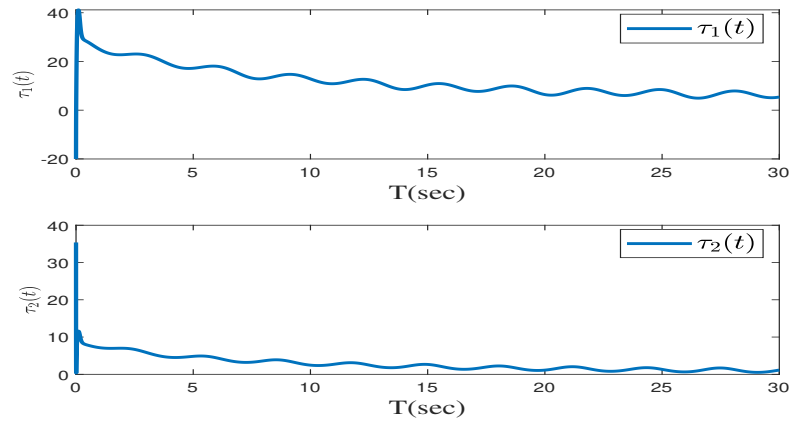


Fig 8. The input control signals.

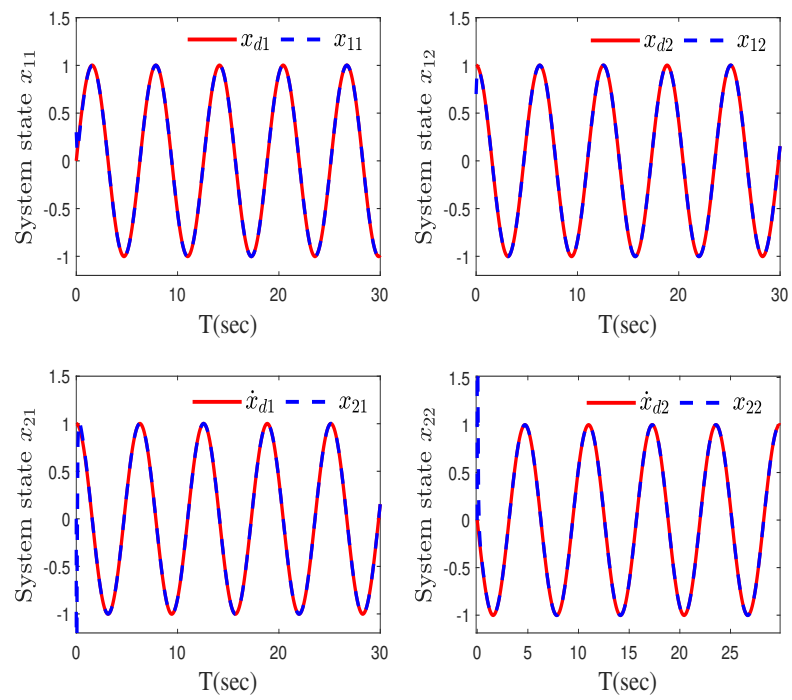


Fig 9. System states.

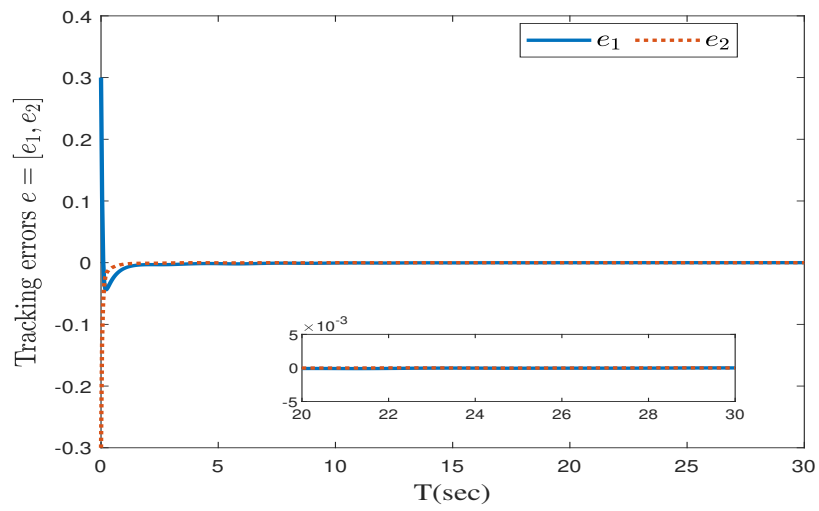


Fig 10. Tracking error e .

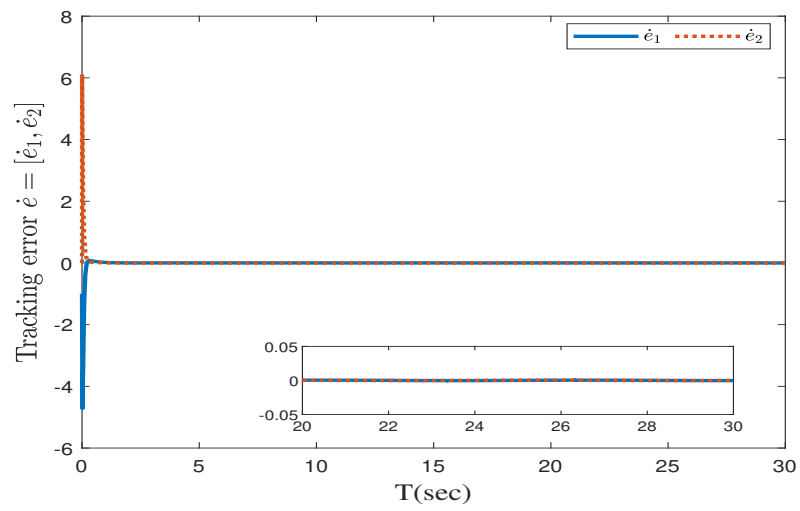


Fig 11. Tracking error \dot{e} .

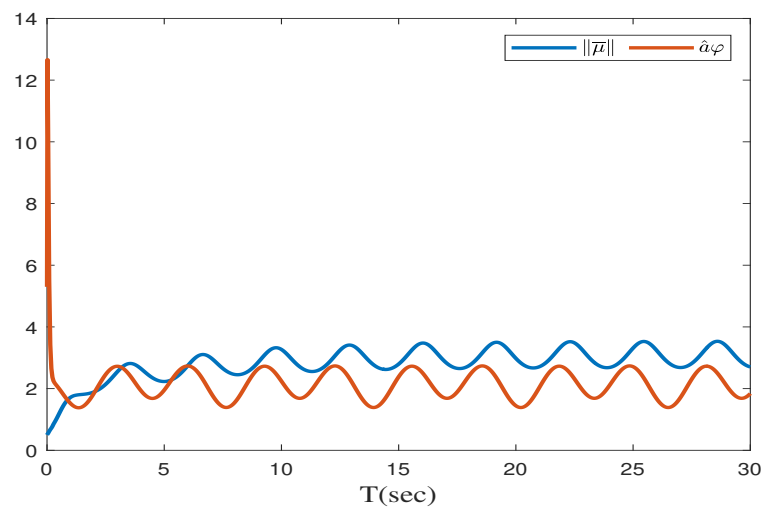


Fig 12. $\bar{\mu}$ and \hat{a}_φ .

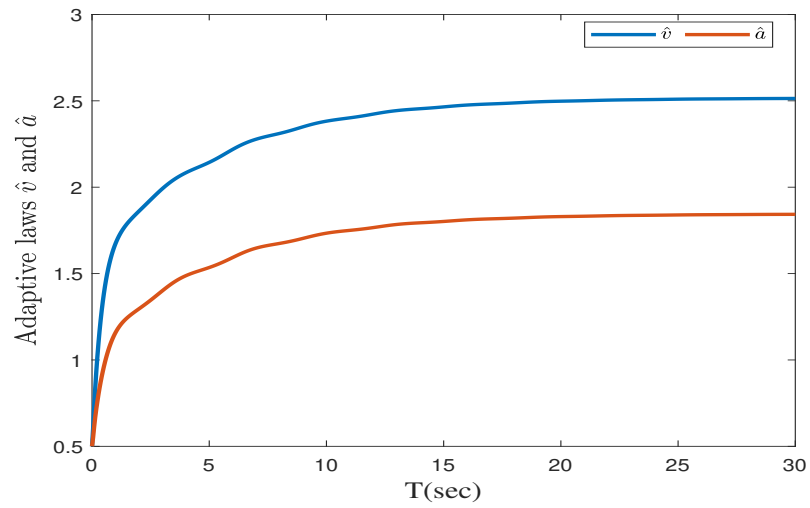


Fig 11. Adaptive parameters.

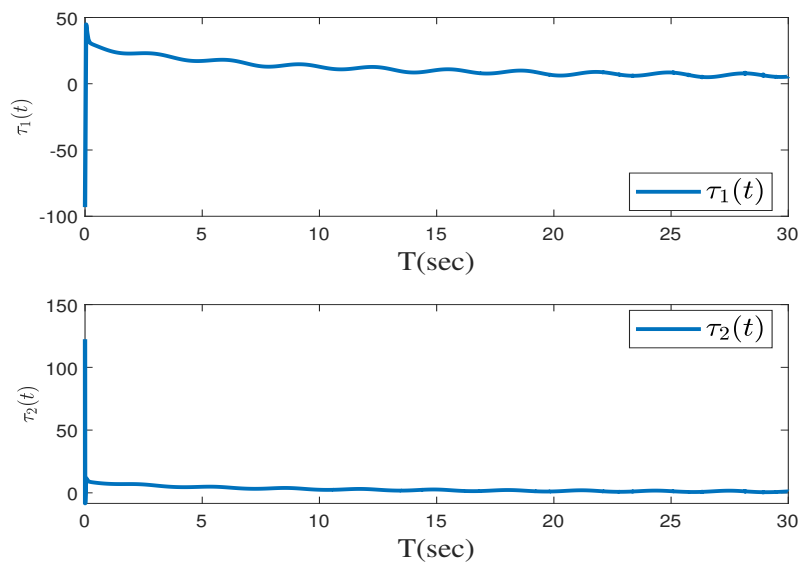


Fig 13. The input control signals.

5. Conclusions

In this paper, we study the backstepping-based control and FV-based control for a 2-link manipulator. The system model under multiple disturbances and uncertainties is established. The proposed control schemes can overcome the lumped uncertainties and multiple disturbances well with the help of NN-based adaptive updating law.

Acknowledgement

This research was not funded by any grant.

Conflicts of Interest

The authors declare no conflicts of interest.

References

- [1] Zheshuo, Z., Bangji, Z., & Yin, H. (2023). Constraint-based adaptive robust tracking control of uncertain articulating crane guaranteeing desired dynamic control performance. *Nonlinear Dynamics*, 111(1), 11261–11274. <https://doi.org/10.1007/s11071-023-08452-4>
- [2] Zhang, Z., Zhang, B., Cao, D., & Yin, H. (2024). Precise tracking control for articulating crane: Prescribed performance, adaptation, and fuzzy optimality by nash game. *IEEE Transactions on Cybernetics*, 54(1), 387–400. <https://doi.org/10.1109/TCYB.2023.3264602>
- [3] Xian, Y., Huang, K., Zhu, Z., Zhen, S., & Chen, Y.-H. (2025). Guaranteeing performance robust control for human-machine systems with optimal human decision. *IEEE Transactions on Cybernetics*, 55(2), 854–866. <https://doi.org/10.1109/TCYB.2024.3500133>
- [4] Hejrati, M., & Mattila, J. (2025a). Orchestrated robust controller for precision control of heavy-duty hydraulic manipulators. *IEEE Transactions on Automation Science and Engineering*, 22, 14284–14305. <https://doi.org/10.1109/TASE.2025.3559595>
- [5] Hejrati, M., & Mattila, J. (2025b). Impact-resilient orchestrated robust controller for heavy-duty hydraulic manipulators. *IEEE/ASME Transactions on Mechatronics*, 1–12. <https://doi.org/10.1109/TMECH.2025.3562395>
- [6] Mattila, J., Koivumäki, J., Caldwell, D. G., & Semini, C. (2017). A survey on control of hydraulic robotic manipulators with projection to future trends. *IEEE/ASME Transactions on Mechatronics*, 22(2), 669–680. <https://doi.org/10.1109/TMECH.2017.2668604>
- [7] Xu, Z., Deng, W., Shen, H., & Yao, J. (2022). Extended-state-observer-based adaptive prescribed performance control for hydraulic systems with full-state constraints. *IEEE/ASME Transactions on Mechatronics*, 27(6), 5615–5625. <https://doi.org/10.1109/TMECH.2022.3186390>
- [8] Mohanty, A., & Yao, B. (2011). Integrated direct/indirect adaptive robust control of hydraulic manipulators with valve deadband. *IEEE/ASME Transactions on Mechatronics*, 16(4), 707–715. <https://doi.org/10.1109/TMECH.2010.2051037>
- [9] Truong, H. V. A., Nam, S., Kim, S., Kim, Y., & Chung, W. K. (2024). Backstepping-sliding-mode-based neural network control for electro-hydraulic actuator subject to completely unknown system dynamics. *IEEE Transactions on Automation Science and Engineering*, 21(4), 6202–6216. <https://doi.org/10.1109/TASE.2023.3323148>
- [10] Mononen, T., Aref, M. M., & Mattila, J. (2019). Nonlinear model predictive control of a heavy-duty hydraulic bulldozer blade. 2019 IEEE International Conference on Cybernetics and Intelligent Systems 565–570. <https://doi.org/10.1109/CIS-RAM47153.2019.9095816>

- [11] Zhao, K., Song, Y., Ma, T., & He, L. (2018). Prescribed performance control of uncertain euler-lagrange systems subject to full-state constraints. *IEEE Transactions on Neural Networks and Learning Systems*, 29(8), 3478–3489. <https://doi.org/10.1109/TNNLS.2017.2727223>
- [12] Yao, Z., Xu, F., Jiang, G.-P., & Yao, J. (2024). Data-driven control of hydraulic manipulators by reinforcement learning. *IEEE/ASME Transactions on Mechatronics*, 29(4), 2673–2684. <https://doi.org/10.1109/TMECH.2023.3336072>
- [13] Liang, X., Yao, Z., Deng, W., & Yao, J. (2025). Adaptive neural network finite-time tracking control for uncertain hydraulic manipulators. *IEEE/ASME Transactions on Mechatronics*, 30(1), 645–656. <https://doi.org/10.1109/TMECH.2024.3396493>
- [14] Zhang, S., Dong, Y., Ouyang, Y., Yin, Z., & Peng, K. (2018). Adaptive neural control for robotic manipulators with output constraints and uncertainties. *IEEE Transactions on Neural Networks and Learning Systems*, 29(11), 5554–5564. <https://doi.org/10.1109/TNNLS.2018.2803827>
- [15] Levin, A., & Narendra, K. (1996). Control of nonlinear dynamical systems using neural networks. ii. observability, identification, and control. *IEEE Transactions on Neural Networks*, 7(1), 30–42. <https://doi.org/10.1109/72.478390>
- [16] Zhang, Z., Song, Y., & Zhao, K. (2019). Neuroadaptive cooperative control without velocity measurement for multiple humanoid robots under full-state constraints. *IEEE Transactions on Industrial Electronics*, 66(4), 2956–2964. <https://doi.org/10.1109/TIE.2018.2844791>
- [17] Sun, W., Wu, Y., & Lv, X. (2022). Adaptive neural network control for full-state constrained robotic manipulator with actuator saturation and time-varying delays. *IEEE Transactions on Neural Networks and Learning Systems*, 33(8), 3331–3342. <https://doi.org/10.1109/TNNLS.2021.3051946>
- [18] Guo, L., Li, W., Zhu, Y., Yu, X., & Wang, Z. (2023). Composite disturbance filtering: A novel state estimation scheme for systems with multisource, heterogeneous, and isomeric disturbances. *IEEE Open Journal of the Industrial Electronics Society*, 4, 387–400. <https://doi.org/10.1109/OJIES.2023.3317271>
- [19] Xi, R.-D., Xiao, X., Ma, T.-N., & Yang, Z.-X. (2022). Adaptive sliding mode disturbance observer based robust control for robot manipulators towards assembly assistance. *IEEE Robotics and Automation Letters*, 7(3), 6139–6146. <https://doi.org/10.1109/LRA.2022.3164448>
- [20] Zhu, Y., Qiao, J., & Guo, L. (2019). Adaptive sliding mode disturbance observer-based composite control with prescribed performance of space manipulators for target capturing. *IEEE Transactions on Industrial Electronics*, 66(3), 1973–1983. <https://doi.org/10.1109/TIE.2028.2838065>
- [21] Habibi, H., Howard, I., Simani, S., & Fekih, A. (2021). Decoupling adaptive sliding mode observer design for wind turbines subject to simultaneous faults in sensors and actuators. *IEEE/CAA Journal of Automatic Control*, 8(4), 837–847. <https://doi.org/10.1109/JAS.2021.1003931>
- [22] Chen, Z., Dawara, A. A., Zhang, X., Zhang, H., Liu, C., & Luo, G. (2022). Adaptive sliding mode observer-based sensorless control for spmsm employing a dual-pll. *IEEE Transactions on Transportation Electrification*, 8(1), 1267–1277. <https://doi.org/10.1109/TTE.2021.3112123>